Polymer 43 (2002) 4033–4041

polymer

www.elsevier.com/locate/polymer

Fracture of polybutylene terephthalate (PBT) film

S. Hashemi*

School of Polymer Technology, University of North London, Holloway Road, London N7 8DB, UK

Received 23 November 2001; accepted 15 March 2002

Abstract

Combined effects of thickness and temperature on essential work of fracture (EWF) of polybutylene terephthalate (PBT) film were studied using single edge notched tension (SENT) and double edge notched tension specimens. It is found that specific essential work of fracture (w_e) for PBT is independent of temperature below T_g (≈80 °C), but decreases above T_g. Between temperatures 25 and 100 °C, w_e was independent of film thickness in the range 0.125–0.375 mm. The specific non-essential work of fracture (βw_p) was temperature and thickness dependent, being greater for the SENT type specimens. Specimen orientation had no influence on w_e but strongly affected βw_p. It was found that βw_p is greater for cracks propagating normal to the extrusion direction as compared to the parallel direction. © 2002 Elsevier Science Ltd. All rights reserved.

Keywords: Polybutylene terephthalate; Essential work of fracture; Double edge notched tension

1. Introduction

It has been well established that brittle failure can be analysed using linear elastic fracture mechanics (LEFM) approach. In this type of analysis, the area in which energy is dissipated near the crack tip is very small, so that the entire specimen is assumed to exhibit Hookean elasticity. As the extent of plastic deformation at the crack increases, the energy dissipation is no longer confined to a small local zone near the crack tip. Consequently, deviations from LEFM become increasingly significant and this type of analysis is no longer an adequate representation of the system.

One method that may be used to quantify fracture toughness of ductile materials is that of essential work of fracture (EWF) proposed by Broberg [1]. EWF defines a fracture parameter called *specific essential work of fracture*, which may be considered a material constant for a given thickness. This method has recently gained popularity owing to its experimental simplicity and has been used to study the fracture behaviour of a wide range of polymeric materials [2–20].

The work presented here is an extension to the author's previous studies [13–15] on polybutylene terephthalate (PBT) film. In this paper the combined effect of temperature and film thickness on EWF is examined as well as specimen geometry and orientation.

2. Essential work of fracture

2.1. The concept

Broberg [1] stated that when ultimate failure of the pre-notched specimens is preceded by extensive yielding and slow crack growth, a toughness parameter called specific essential work of fracture, w_e, may be evaluated.

Following Broberg's idea, Cotterell and Reddel [21] proposed that the non-elastic region at the crack tip comprises two zones as depicted in Fig. 1(a); an inner fracture process zone (IFPZ), where fracture actually takes place; and an outer plastic deformation zone (OPDZ), where plastic deformation is necessary to accommodate the strain in the end region. Based on this concept, total work of fracture, W_t, given by the area under load–displacement ($P-\delta$) curve, is partitioned into two components.

2.1.1. Essential work of fracture, W_e

This is the work expended in the IFPZ by neck formation and tearing. W_e is a surface energy term whose value is proportional to the ligament area (LB), i.e.

$$W_e = w_e BL \quad (1)$$

w_e is called specific essential work of fracture and is considered to be a material constant for a given thickness.

* Tel.: +44-207-7535128; fax: +44-7535081.
E-mail address: s.hashemi@unl.ac.uk (S. Hashemi).

PII: S0032-3861(02)00204-5

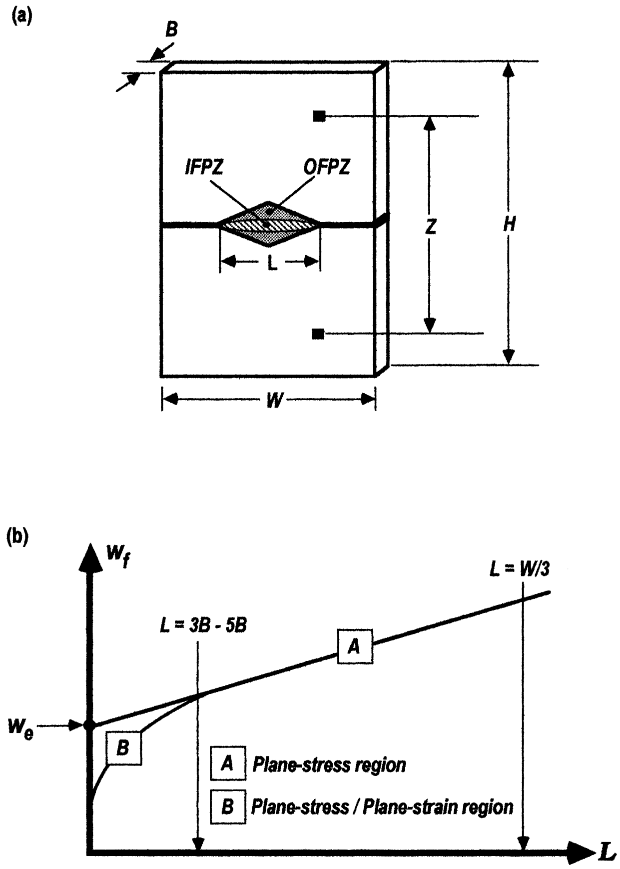

Fig. 1. (a) Schematic representation of the IFPZ and the OPDZ. (b) Schematic representation of the specific total work of fracture versus ligament length.

2.1.2. Non-essential work of fracture, W_p

This is the work dissipated in the OPDZ, where various types of deformation such as shear yielding and microvoiding may be operating. If it is assumed that W_p is proportional to the volume of yielded zone V_p (L, B), then

$$W_p = w_p V_p(L, B) \tag{2}$$

where w_p is called specific non-essential work of fracture (NEWF). It is further assumed that $V_p(L, B)$ is proportional to BL^2 with proportionality constant β that is independent of the ligament length, i.e.

$$W_p = w_p \beta B L^2 \tag{3}$$

where β is the plastic zone shape factor whose value depends on the geometry of the specimen and the crack.

In terms of specific work terms, we may write

$$w_t = \frac{W_t}{LB} = w_e + \beta w_p L \tag{4}$$

where w_t is termed the specific total work of fracture.

According to Eq. (4) parameters w_e and βw_p can be evaluated by linearly interpolating the experimental data of w_t versus L. The positive intercept of the regression line at $L = 0$ gives w_e and the slope gives βw_p, as shown schematically in Fig. 1(b).

The physical meaning of w_e can be interpreted by taking a contour integral around the edge of a fully developed fracture process zone of length ρ and width d formed at the crack tip. The term w_e is then considered as that work which is dissipated in the fracture process zone at the crack tip. This includes; (i) the plastic work up to necking in the material that is to form the process zone, w_{eI} and (ii) the work to fracture the neck, w_{eII}. Assuming, there is uniform straining up to necking, we may write

$$w_{eI} = d \int_0^{\bar{e}_n} \bar{\sigma}\, d\bar{e} \tag{5}$$

where $\bar{\sigma}$ and $\bar{e}$ are the true stress and strain, respectively, and $\bar{e}_n$ is the true strain at necking (note that $\int \bar{\sigma}\, d\bar{e}$ is the local strain energy density). After necking, the deformation in the process zone is localised and non-uniform. If it is assumed that fracture occurs when crack tip is further stretched so that crack opening displacement (δ) has reached a critical value, δ_c

$$w_{eII} = \int_{de_n}^{\delta_c} \sigma(\delta) d\delta \tag{6}$$

where $\bar{\sigma}$ and e_n are the engineering stress and strain at necking, respectively.

By summing the two integrals we obtain:

$$w_e = d \int_0^{\bar{e}_n} \bar{\sigma}\, d\bar{e} + \int_{e_n d}^{\delta_c} \sigma(\delta) d\delta \tag{7}$$

Since d and δ_c are expected to vary with thickness, then according to Eq. (7), w_e should also vary with thickness. For this reason, w_e is regarded to be a material constant, only, for a given thickness.

2.2. Data reduction scheme

It must be realised that EWF approach is based on four key assumptions:

(i) Geometrical similarity exists between specimens of different ligament lengths during crack growth.
(ii) Ligament length is fully yielded prior to the onset of crack propagation.
(iii) Ligament length controls the size of the OPDZ and the volume of the zone is proportional to the square of the ligament length.
(iv) Fracture occurs under pure plane-stress conditions for which w_e and βw_p are both independent of the ligament length.

To satisfy these assumptions and maintain linearity of w_t with L as expressed by Eq. (4), it has been recommended that ligament length should meet the following pre-requisites [22]:

(i) $L \leq 2R_p$: This ensures that complete yielding of the

ligament region occurs prior to crack growth, hence maintaining the proportionality of W_p and L^2. R_p is the radius of the plastic zone at the crack tip.
(ii) $L \leq W/3$: This ensures that the size of the plastic zone is not disturbed by the lateral boundaries of the test specimen (edge effects) and therefore plastic deformation is confined to the ligament area.
(iii) $L \geq 3B$–$5B$: This ensures that the state of stress in the ligament region is one of pure plane stress and not mixed mode in which case stress state will have both plane-stress and plane-strain characteristics. This leads to non-linearly in w_t versus L plot as depicted in Fig. 1(b) as both w_e and w_p terms become ligament length dependent.

These restrictions on L, in effect, defines the valid ligament length range for plane-stress determination of w_e as [22]

$$L_{min} = 3B\text{–}5B, \qquad L_{max} = \min\left(\frac{W}{3}, 2R_p\right) \tag{8}$$

where L_{min} and L_{max} are, respectively, the minimum and maximum ligament length threshold values. The length $2R_p$ can be estimated from the following equation

$$2R_p = \frac{1}{\pi}\frac{Ew_e}{\sigma_y^2} \tag{9}$$

where E is the Young's modulus and σ_y is the uniaxial tensile yield stress of the material.

The minimum ligament length, L_{min} may be verified experimentally by plotting the maximum net-section stress, σ_n, obtained during the test (maximum load on the load–displacement curve divided by the ligament area, LB) against the ligament length, L. In such a plot, two regions may be identified:

(i) A plane-stress region in which σ_n is independent of ligament length. According to analysis by Hill [23], $\sigma_n = \sigma_y$ for single edge notched tension (SENT) and $\sigma_n = 1.15\sigma_y$ for double edge notched tension (DENT) type specimens, in this region. It must be said, however, that for each specimen type, values greater and smaller than the theoretical value have also been obtained experimentally [6,8,9,11,13–15,17,19,20]. Indeed, it is nowadays believed that so long as failure of the specimens is by ductile tearing of the ligament region, the EWF analysis should still be applicable whatever may be the value of σ_n.
(ii) A plane-stress/plane-strain region, often referred to as mixed mode region, in which σ_n increases with decreasing ligament length.

It should therefore be possible in practice to determine the length L_{min} from the plot of σ_n versus L and to exclude data points for which $L < L_{min}$ from regression analysis to be performed on w_t versus L plot.

It is worth stating at this stage, that although the prescribed length for L_{min} is $3B$–$5B$, higher values have been reported for polymeric films [2,8,11,13–17,19,20]. It has also been found that L_{min} is material dependent and therefore has no universal value as originally thought.

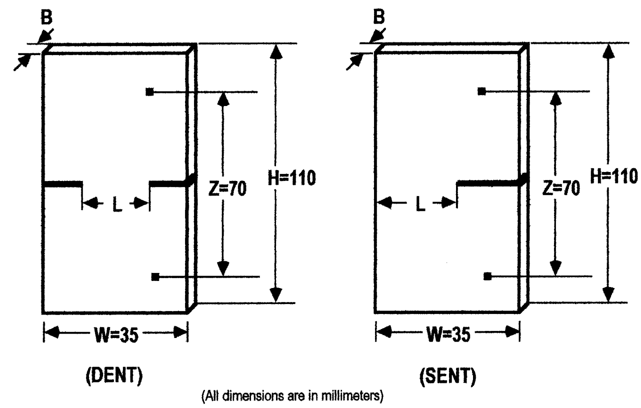

Fig. 2. SENT and DENT specimens.

3. Experimental details

This study was conducted on semi-crystalline PBT films having nominal thickness values of 125, 175, 375 and 500 μm, crystallinity of about 41% and glass transition temperature (T_g) of ≈80 °C.

EWF measurements were carried out between 23 and 100 °C on rectangular coupons having a constant width (W) of 35 mm and overall length (H) of 105 mm. The coupons were cut from sheets such that the longitudinal axis of the coupon was either parallel (MD) or perpendicular (TD) to the extrusion direction. The coupons were then notched to produce series of DENT and SENT specimens with ligament length (L) ranging from 5 to 20 mm as shown in Fig. 2. The initial notch in MD specimens was perpendicular to the extrusion direction and in TD specimens along the extrusion direction. After notching specimens were then tested in an Instron testing machine at a constant crosshead displacement rate of 5 mm/min using pneumatic clamps with initial separation (Z) of 70 mm. The load–displacement (P–δ) curves, typical examples of which are given in Fig. 3(a)–(d), were recorded using a computer data logger.

Additionally, tensile yield stress (σ_y) and modulus (E) were measured using dumbbell-shaped specimens. The load–displacement curves typical examples of which are shown in Fig. 4 as a function of test temperature exhibit straining softening and cold-drawing phenomenon before failure. From the initial slope and maximum load on the P–δ curves, values of E and σ_y were, respectively, calculated. As expected, σ_y and E both decreased with increasing temperature and by and large were independent of specimen thickness. The values obtained via MD specimens were 10–15% higher than the TD specimens.

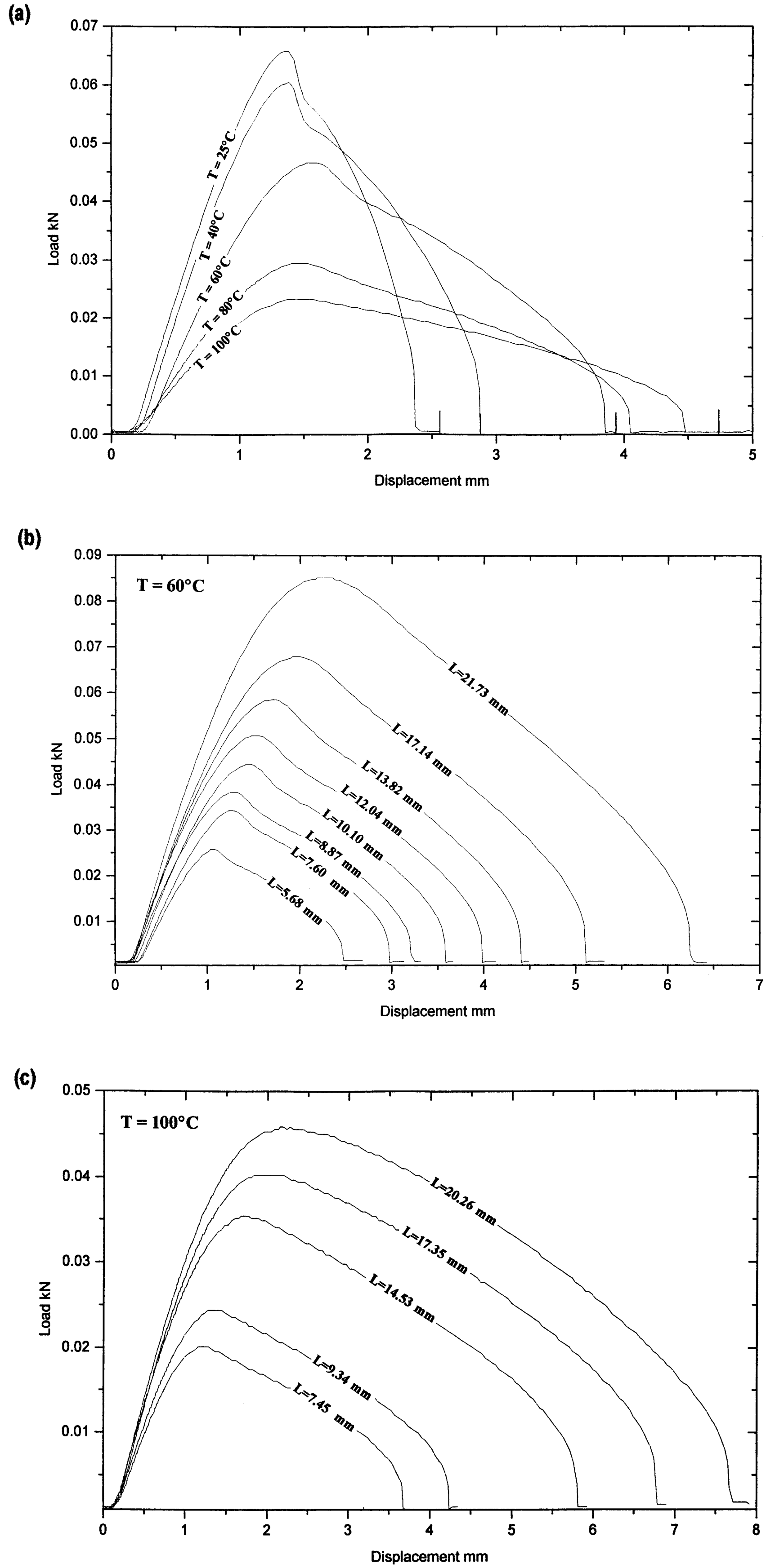

Fig. 3. Typical EWF load–displacement curves: (a) DENT specimens between 25 and 100 °C ($B = 125$ μm, $L = 10$ mm). (b) DENT specimens with different L values at 60 °C ($B = 125$ μm). (c) DENT specimens with different L values at 100 °C ($B = 125$ μm). (d) DENT and SENT specimens at $B = 375$ μm, $L = 10$ mm.

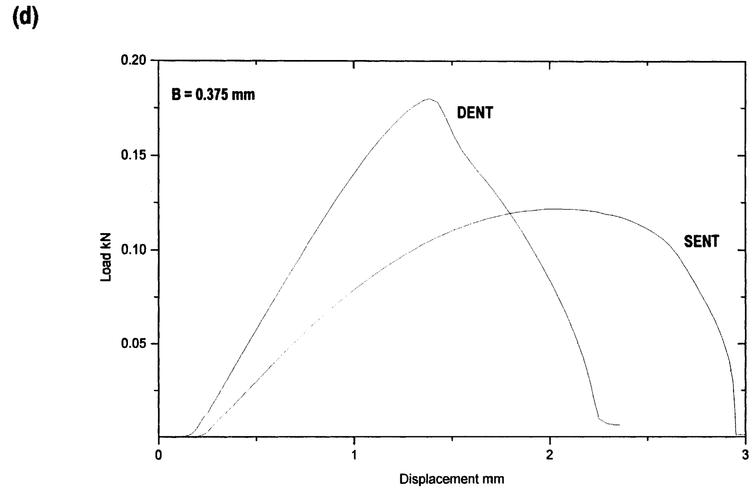

Fig. 3. (*continued*)

4. Results and discussion

4.1. Fracture behaviour

Failure of the DENT and SENT specimens was always stable and occurred after crack tip yielding which appeared as stress-whitened region as shown in Fig. 5. The progressive development of the stress-whitened region led to full yielding of the ligament region prior to failure in both specimen types. However, whilst full yielding of the ligament region in DENT specimens occurred at maximum load, in the case of SENT specimens, this occurred after maximum load was reached. The necking down of the fully yielded ligament region in DENT specimens led to a prominent load-drop after maximum for $T < T_g$ as it is evident from the load–displacement curves in Fig. 3. The following observations were also made:

(i) General behaviour of the $P-\delta$ curves and the way in which DENT and SENT specimens fractured were by and large unaffected by the test variables.
(ii) For a given specimen geometry, load–displacement curves were geometrically similar to one another for different ligament lengths.

Bearing in mind that propagation of the crack in DENT type specimens occurred after full yielding of the ligament region, it can be said that at least two of the four key assumptions were met by DENT specimens, if not by the SENT specimens.

4.2. Effect of specimen orientation on EWF parameters

This study was performed at 25 °C on SENT type

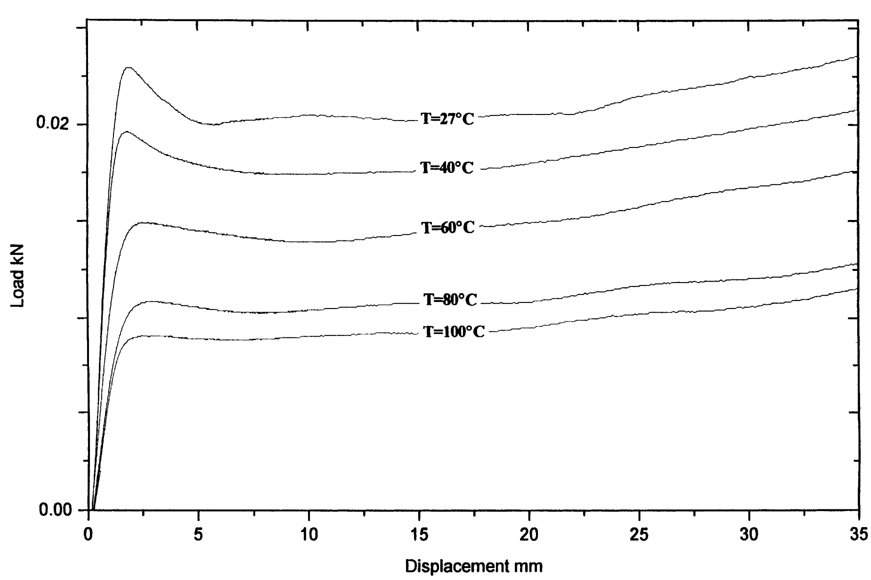

Fig. 4. Typical tensile load–displacement curves as a function of test temperatures ($B = 125$ μm).

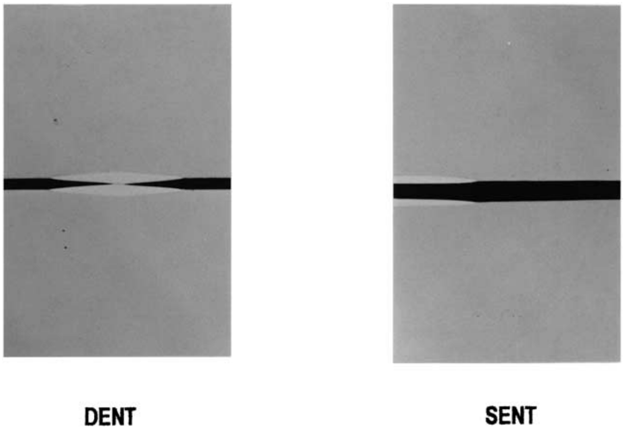

Fig. 5. Typical DENT and SENT fractured specimens at 25 °C.

specimens having thickness (B) values of 125, 175, 275 and 500 μm.

Fig. 6 shows that variation of σ_n with L follows the trend described earlier. It can be seen that although specimen thickness has no great influence upon σ_n, specimen orientation tends to affect σ_n with MD specimens exhibiting a higher value (≈37 MPa) than TD specimens (≈33 MPa). Fig. 6 further shows that plane-stress/plane-strain transition for both MD and TD specimens occurs at a ligament length value (L_{min}) of about 8–10 mm. This corresponds to transitional ratio (i.e. L_{min}/B) in the range of 64–16, as specimen thickness is increased from 125 to 500 μm. This observation corroborates with previous findings in confirming that the transition in polymeric films is much greater than 3–5 and has no universal value.

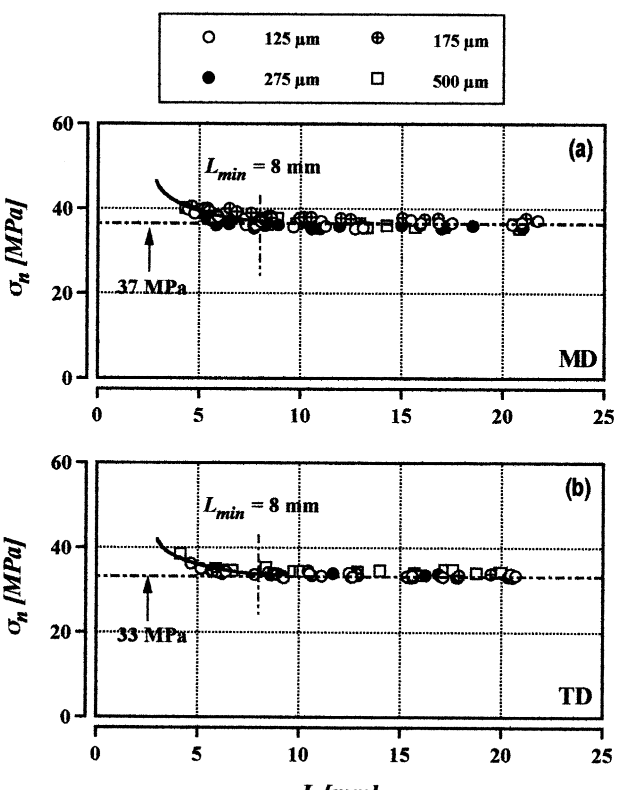

Fig. 6. Effect of specimen orientation on net-section stress versus ligament length at 25 °C for SENT specimens of various thicknesses; (a) MD and (b) TD.

Fig. 7 shows the effect of specimen orientation on total work of fracture (w_t) versus ligament length (L), for the range of thickness values studies here. It is seen that variation is linear over the entire ligament length range under consideration and therefore unlike σ_n versus L plots, show no strong evidence of a plane-stress/plane strain region when $L < L_{min}$. This observation suggests that increase in net-section stress was presumably not significantly large enough to affect linearity of w_t with L. There is also no clear indication that w_t values have been affected in any significant way by the specimen boundaries, as L exceeding the length $W/3$ (≈11.67 mm).

Plots in Fig. 7 further reveal:

(i) Total work of fracture, w_t, is affected by orientation, being greater for cracks propagating normal to the extrusion direction compared to the parallel direction. This is attributed to MD specimens having the greater elongation and load values.
(ii) Slope of the line w_t versus L, representing the specific NEWF, βw_p, is greater for cracks propagating normal to the extrusion direction (MD specimens) as opposed to when propagating along the extrusion direction (TD specimens).
(iii) Intercept value of the line w_t versus L at zero ligament length, representing the specific essential work of fracture, w_e, is independent of both thickness and orientation. The idea that w_e is a material constant for a given thickness, therefore is not supported by the results obtained in this study. In view of Eq. (7), it may be said that thickness must have had no major influence upon the width of the process zone and the crack opening displacement within the process zone.

Finally, taking $w_e \approx 36.46$ kJ/m^2, we calculated the length $2R_p$ for MD and TD specimens using Eq. (9). Inserting in Eq. (9) values of $\sigma_y = 46.35$ MPa and $E = 2.43$ GPa for MD and $\sigma_y = 41$ MPa and $E = 2.20$ GPa for TD, give $2R_p = 13.13$ mm for MD and $2R_p = 15.19$ mm for TD specimens, i.e. $2R_p > W/3$, in both cases.

4.3. Combined effect of specimen thickness and temperature on EWF

Series of DENT type specimens with MD orientation and thickness values of 125, 175 and 375 μm were tested between 25 and 100 °C.

Fig. 8 shows that whilst σ_n is not greatly influenced by thickness of the specimens, it decreases with increasing temperature and rises on diminishing L. It can be seen that plane-stress/plane-strain transition occurs at $L_{min} \approx 10$ mm,

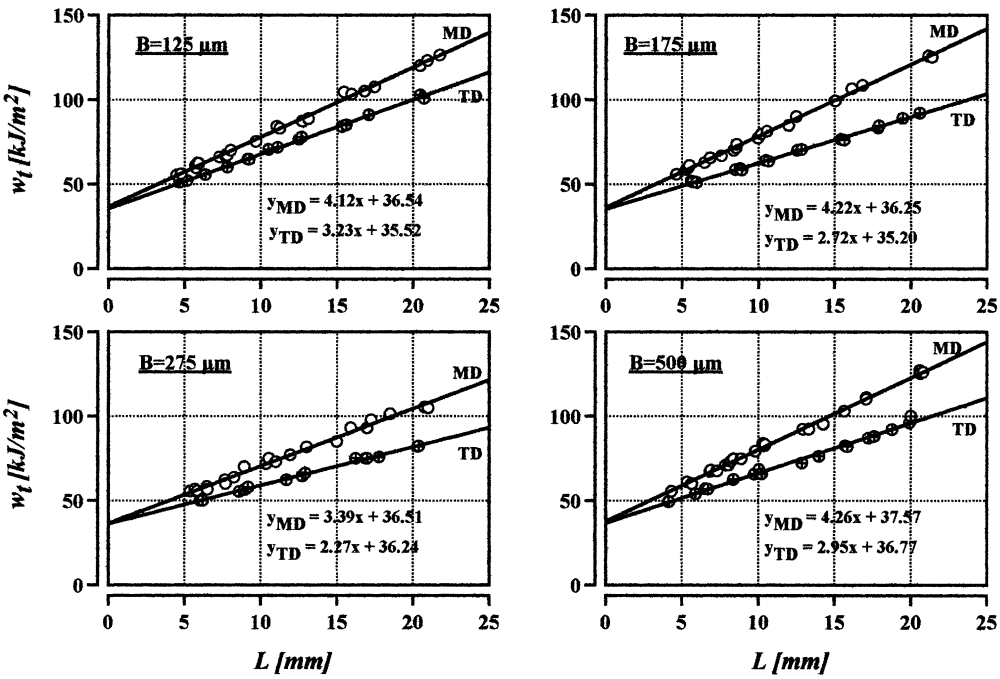

Fig. 7. Effect of specimen orientation on specific total work of fracture versus ligament length at 25 °C for SENT type specimens of various s thicknesses.

in all cases, i.e. being independent of test variables. It is also seen that when test temperature exceeds 25 °C, $\sigma_n \approx 1.15\sigma_y$, as predicted by Hill [23].

Variation of the specific total work of fracture (w_t) with ligament length (L) between 25 and 100 °C for each thickness can be found in Fig. 9(a)–(c). It is seen that plots are predominantly linear over the entire ligament length range and therefore the pre-requisite $L_{max} < \min(2R_p, W/3)$ bears no relation to the results obtained in this study. The intercept values at $L = 0$ (i.e. w_e) are plotted against temperature in Fig. 10(a) where it can be seen that w_e is independent of

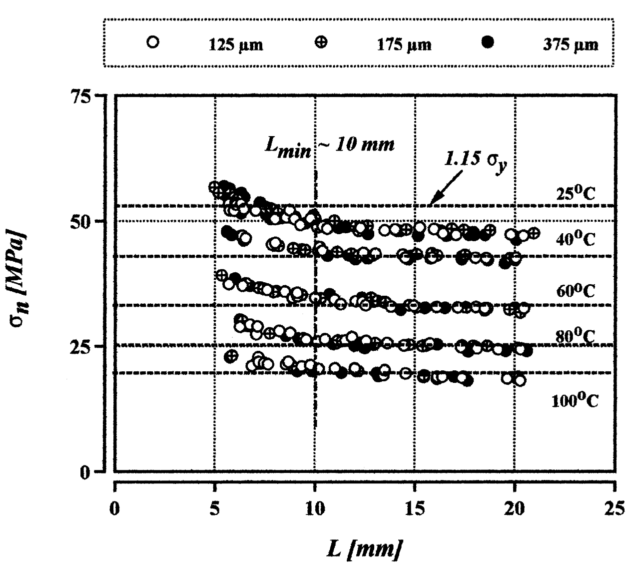

Fig. 8. Effect of specimen thickness and temperature on net-section stress versus ligament for DENT type specimens.

temperature for $T \leq T_g$ but tends to decrease above T_g. However, over the entire temperature range under consideration, w_e remains very much independent of thickness.

The previous studies [6,8,9,11,17,20], have shown that w_e can be estimated reasonably well using the crack opening displacement approach. This approach entails using a relationship of the form $w_e = \sigma_y \delta_c$, where σ_y is the tensile yield stress and δ_c is the critical value of the crack opening displacement. As values of σ_y and δ_c change with increasing temperature, with the latter increasing and the former decreasing, the observed temperature dependence of w_e is explained here in terms of σ_y and δ_c competing:

- $T \leq T_g$: Decrease in σ_y with increasing temperature is compensated by the increase in δ_c, i.e. temperature independent w_e.
- $T > T_g$: Decrease in σ_y with increasing temperature outweighs the increase in δ_c, i.e. decreasing w_e.

From the slope of the lines in Fig. 9(a)–(c), specific NEWF (βw_p) values were determined. It is seen from Fig. 10(b) that βw_p is temperature dependent and has a maximum in the vicinity of T_g. It is also seen that βw_p decreases with thickness over the entire temperature range under consideration.

Finally, $2R_p$ was calculated as a function of temperature using Eq. (9). The calculated values were either close to or they were greater than the length $W/3$. However, bearing in mind that ligament length in all DENT specimens were fully yielded prior to the propagation of the crack, the pre-requisite $L < 2R_p$ seems restrictive, in this case.

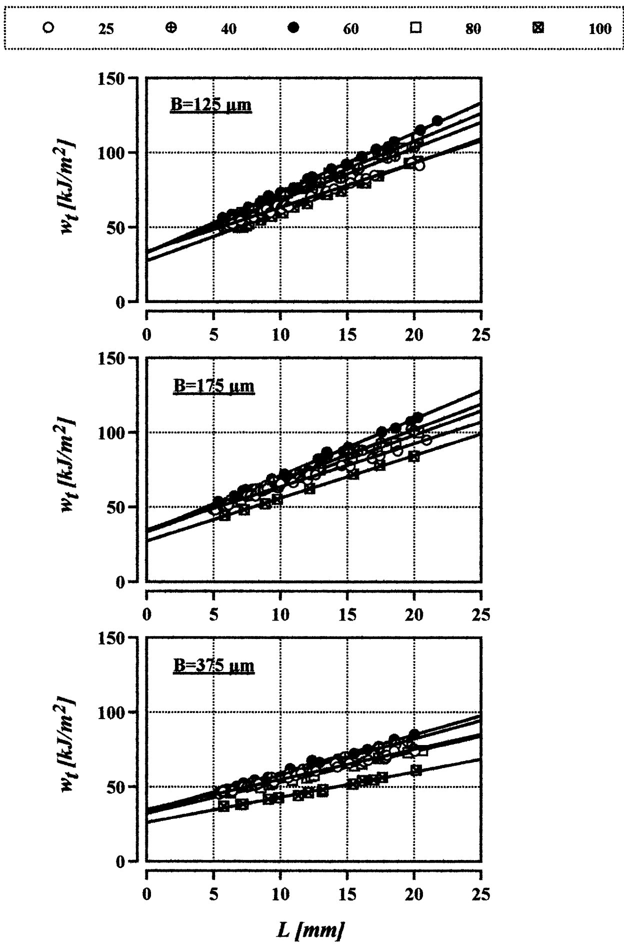

Fig. 9. Effect of temperature on specific total work of fracture versus ligament length for DENT type specimens having thickness values of 125, 175 and 375 μm.

4.4. Effect of specimen geometry on EWF

A series of SENT specimens (MD orientation) having thickness of 175 μm were tested between 25 and 100 °C.

It is seen from Fig. 11(a) that stress-state transition occurs at $L_{min} \approx 10$ mm and that above this ligament length, $\sigma_n \approx \sigma_y$, as predicted by Hill [23].

Fig. 11(b) shows variation of w_t with L for SENT specimens between 25 and 100 °C. It is seen that variation is predominantly linear over the entire ligament length and temperature range. For comparative purposes, values of w_e and βw_p for the two types of specimen are given in Table 1. It can be observed, that w_e values are comparable; but, βw_p values for SENT specimens are significantly higher. As is often reported, this behaviour arises due to the differences in shape of the OPDZ, in the two types of specimen.

5. Conclusions

The effect of specimen thickness, orientation and geometry and temperature on essential and NEWF parameters for PBT film was studied. Results indicated:

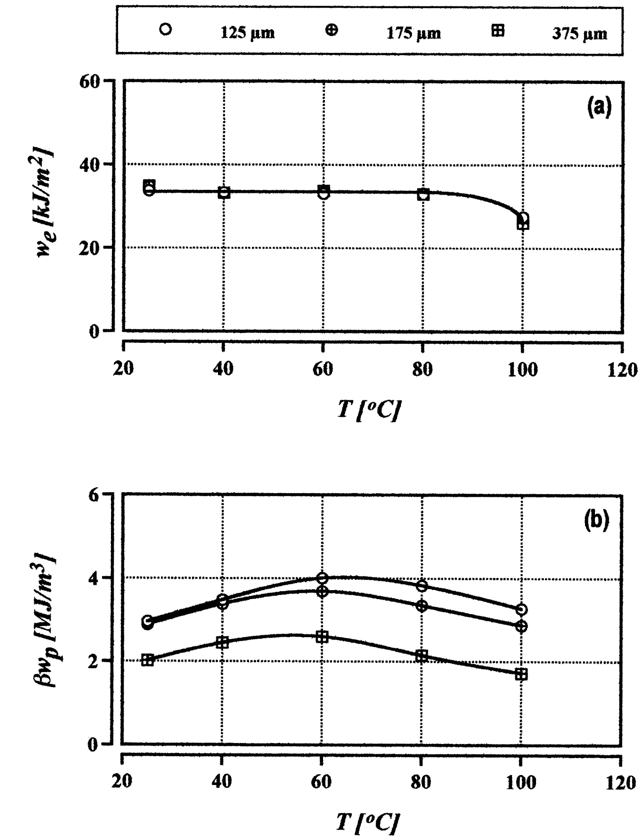

Fig. 10. (a) Specific essential work of fracture versus temperature for DENT type specimens of various thicknesses.

(i) Between 25 and 100 °C, specific essential work of fracture (w_e) is independent of thickness. Within the same temperature range, specific NEWF (βw_p) is thickness dependent.
(ii) w_e is independent of test temperature below T_g (≈80 °C), but decreases above T_g. The βw_p parameter is temperature dependent, showing a maximum near T_g.
(iii) w_e is not affected by the specimen orientation. However, specific NEWF is influenced strongly by orientation, being greater for cracks propagating normal to the extrusion direction as compared to the parallel direction.
(iv) w_e values obtained via SENT and DENT type specimens were comparable; but, βw_p values for SENT specimens were significantly higher.

Table 1
Work of fracture parameters for SENT and DENT specimens (B = 0.175 μm)

Temperature (°C)	w_e (kJ/m^2)		βw_p (kJ/m^3)	
	SENT	DENT	SENT	DENT
25	36.25	34.79	4.22	2.89
60	37.66	33.35	6.79	3.79
80	36.06	33.18	5.44	3.26
100	26.16	27.37	4.00	2.87

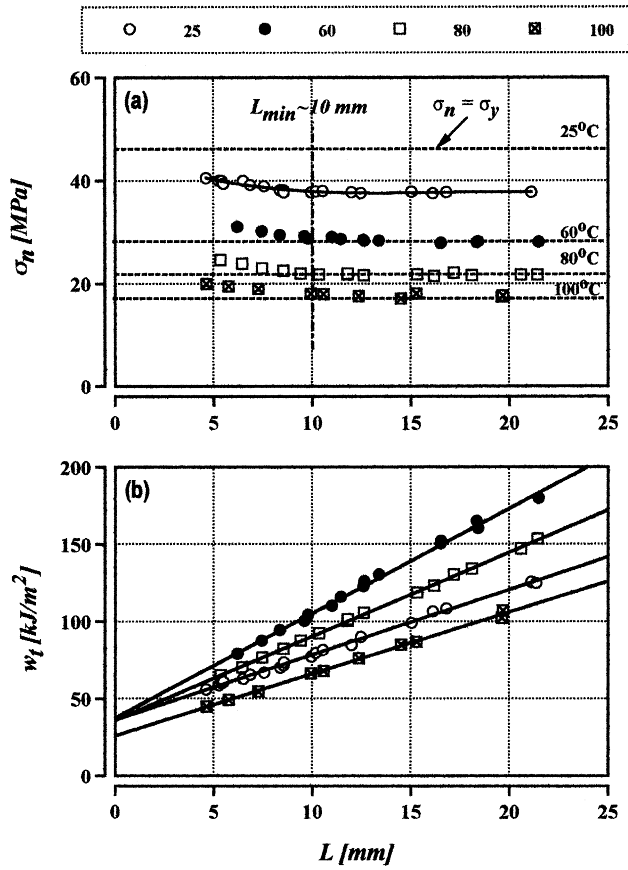

Fig. 11. (a) Effect of temperature on net-section versus ligament for SENT type specimens of thickness 175 μm. (b) Effect of temperature on specific total work of fracture versus ligament for SENT type specimen of thickness 175 μm.

References

[1] Broberg KB. Int J Fract 1968;4:11.
[2] Mai YW, Cotterell B, Horlyck R, Vigna G. Polym Engng Sci 1987;27:804.
[3] Paton CA, Hashemi S. J Mater Sci 1992;27:2279.
[4] Wu J, Mai YW, Cotterell B. J Mater Sci 1993;28:3373.
[5] Chan WYF, Williams JG. Polymer 1994;35:1666.
[6] Wu J, Mai YW. Polym Engng Sci 1996;36:2275.
[7] Karger-Kocsis J, Czigany T. Polymer 1996;37:2433.
[8] Hashemi S. J Mater Sci 1997;32:1573.
[9] Karger-Kocsis J, Czigany T, Moskala EJ. Polymer 1997;38:4587.
[10] Karger-Kocsis J, Czigany T, Moskala EJ. Polymer 1998;39:3939.
[11] Arkhireyeva A, Hashemi S, O'Brien M. J Mater Sci 1999;34:5961.
[12] Ferrer-Balas D, Maspoch ML, Martinez AB, Santana OO. Polym Bull 1999;42:101.
[13] Hashemi S. Polym Engng Sci 2000;40:132.
[14] Hashemi S. Polym Engng Sci 2000;40:798.
[15] Hashemi S. Polym Engng Sci 2000;40:1435.
[16] Ching ECY, Li RKY, Mai YW. Polym Engng Sci 2000;40:310.
[17] Hashemi S, Williams JG. Plast Rub Compos 2000;29:294.
[18] Mouzakis DE, Karger-Kocsis J, Moskala EJ. J Mater Sci Lett 2000;19:1615.
[19] Arkhireyeva A, Hashemi S. Plast Rub Compos 2001;30:125.
[20] Arkhireyeva A, Hashemi S. Plast Rub Compos 2001;30:337.
[21] Cotterell R, Reddel JK. Int J Fract 1977;13:267.
[22] Test protocol for essential work of fracture, Version 5, ESIS TC-4 Group, Les Diablerets, 1998.
[23] Hill RH. J Mech Phys Solids 1952;1:19.